trix equation actually solved (compressed matrix) in comparison to the original full-size matrix. Figs. 3 and 4 show the electric field at various time steps after the fifth (640 out of 8192 basis functions and compression of 92%) and fifteenth iterations (1920 out of 8192 basis functions and compression of 77%), respectively, together with the reference result E_x^{REF}.

Finally, for comparative purposes, Fig. 5 illustrates a few results obtained using the explicit scheme (dashed line). Obviously, the explicit scheme does not yield the right solution (solid line). The results given here are for a shorter time duration than displayed in Figs. 3 and 4. This duration is limited because the explicit solution very soon becomes unstable. Also, the time intervals between successive graphs are shorter than in Figs. 3 and 4. This is done in order to illustrate in more detail the inherent lag of the explicit solution behind the right one.

IV. Summary and Conclusions

A wavelet-based MoM analysis of an implicit TDIE formulation for the problem of electromagnetic pulse interaction with an air layer in a dielectric medium has been presented. We have demonstrated the inadequacy of the explicit formulation in this case, and have showed that only the implicit formulation is the proper one for analyzing the problem at hand. In addition, the solution has been augmented by applying the IMC method. This is a stable iterative procedure, whereby the solution accuracy, at every spatial location and simultaneously at all the times of interest, is gradually refined.

Acknowledgment

The authors would like to thank Prof. E. Heyman, Tel-Aviv University, Tel-Aviv, Israel, for valuable discussions.

References

[1] K. S. Nikita, G. D. Mitsis, and N. K. Uzunoglu, "Analysis of focusing of pulsed baseband signals inside a layered tissue medium," *IEEE Trans. Microwave Theory Tech.*, vol. 48, pp. 30–39, Jan. 2000.

[2] T. K. Lee, S. Y. Kim, and J. W. Ra, "Diffraction pattern due to a trapezoidal air cylinder in a dielectric," *Microwave Opt. Technol. Lett.*, vol. 27, no. 2, pp. 140–144, Oct. 2000.

[3] J. C. Bolomey, C. Durix, and D. Lesselier, "Time domain integral equation approach for inhomogeneous and dispersive slab problems," *IEEE Trans. Antennas Propagat.*, vol. AP-26, pp. 658–667, Sept. 1978.

[4] A. G. Tijhuis, "Iterative determination of permittivity and conductivity profiles of a dielectric slab in time domain," *IEEE Trans. Antennas Propagat.*, vol. AP-29, pp. 239–245, Mar. 1981.

[5] ——, "PIER 5: Application of conjugate-gradient methods in electromagnetic and signal analysis," in *Iterative Techniques for the Solution of Integral Equations in Transient Electromagnetic Scattering*. Amsterdam, The Netherlands: Elsevier, 1991, ch. 13, pp. 455–538.

[6] R. Mittra, "Topics in applied physics, transient EM fields," in *Integral Equation Methods for Transient Scattering*. Berlin, Germany: Springer-Verlag, 1976, pp. 73–128.

[7] E. K. Miller, "Time domain modeling in electromagnetics," *J. Elect. Waves Applicat.*, vol. 8, no. 9/10, pp. 1125–1172, 1994.

[8] S. M. Rao and T. K. Sarkar, "Time-domain modeling of two-dimensional conducting cylinders utilizing an implicit scheme—TM incident," *Microwave Opt. Technol. Lett.*, vol. 15, no. 6, pp. 342–347, Aug. 1997.

[9] S. J. Dodson, S. P. Walker, and M. J. Bluck, "Implicitness and stability of time domain integral equation scattering analysis," *ACES J.*, vol. 13, no. 3, pp. 291–301, November 1998.

[10] Z. Baharav and Y. Leviatan, "Impedance matrix compression (IMC) using iteratively selected wavelet-basis," *IEEE Trans. Antennas Propagat.*, vol. AP-46, pp. 226–233, Feb. 1998.

[11] ——, "Wavelets in electromagnetics: The impedance matrix compression (IMC) method," *Int. J. Numer. Modeling*, vol. 11, pp. 69–84, Feb. 1998.

[12] Y. Shifman and Y. Leviatan, "On the use of spatio–temporal multiresolution analysis in method of moments solutions for the time-domain integral equation," *IEEE Trans. Antennas Propagat.*, vol. 49, pp. 1123–1129, Aug. 2001.

[13] R. F. Harrington, *Field Computation by Moment Methods*. New York: Macmillan, 1968.

[14] I. Daubechies, *Ten Lectures on Wavelets*. Philadelphia, PA: SIAM, 1992.

[15] G. Strang and T. Nguyen, *Wavelets and Filter Banks*. Cambridge, MA: Wellesley–Cambridge, 1996.

Investigation of Static and Quasi-Static Fields Inherent to the Pulsed FDTD Method

Rolando Pontalti, Jacek Nadobny, Peter Wust, Alessandro Vaccari, and Dennis Sullivan

***Abstract*—This paper demonstrates that trailing dc offsets, which can affect $\mathbf{E}$- or $\mathbf{H}$-fields in finite-difference time-domain simulations, are physically correct static solutions of Maxwell's equations instead of being numerically induced artifacts. It is shown that they are present on the grid when sources are used, which generates nondecaying charges. Static solutions are investigated by exciting electric and magnetic dipoles models with suitable waveforms.**

***Index Terms*—Divergence, FDTD method, Hertzian dipole, infinitesimal current element, triple cosine.**

I. Introduction

The pulsed finite-difference time-domain (FDTD) method [1] is based on a transitory system excitation coupled with the Fourier transform of its response. Excitation is introduced either by "soft" (added) or "hard" (fixed) sources [2]. We use soft sources to model elementary (or Hertzian) electric $\mathbf{p}$ and magnetic $\mathbf{m}$ time-varying dipoles, and compare FDTD results with the analytic solutions, in the static and quasi-static cases.

II. Static Fields in FDTD

The FDTD algorithm solves an initial boundary-value problem using only Maxwell's curl equations. Let us investigate briefly the way in which these vector equations determine the fields' temporal behavior. To this end, we need to study the divergence of $\mathbf{B}$ and $\mathbf{D}$, assuming sources defined as an impressed current density term $\mathbf{J}_s$ in the $\nabla \times \mathbf{H}$ equation. Taking the divergence of both sides of the curl equations, with the initial values $(\nabla \cdot \mathbf{B})_{t=0} \equiv 0$ and $(\nabla \cdot \mathbf{D})_{t=0} \equiv 0$, we notice the following.

Manuscript received May 2, 2001. This work was supported in part by the Italian Ministry for University and Scientific and Technological Research, and in part by the Deutsche Forschungsgemeinschaft.

R. Pontalti and A. Vaccari are with the Istituto Trentino di Cultura, Trento I-38050, Italy.

J. Nadobny is with the Konrad-Zuse-Zentrum für Informationstechnik Berlin, D-14195 Berlin, Germany and is also with the Center of Radiation Medicine, Charité Medical School, Humboldt University of Berlin, D-10099 Berlin, Germany.

P. Wust is with the Center of Radiation Medicine, Charité Medical School, Humboldt University of Berlin, D-10099 Berlin, Germany.

D. Sullivan is with the Department of Electrical Engineering, University of Idaho, Moscow, ID 83843 USA.

Publisher Item Identifier 10.1109/TMTT.2002.801381.

- $\nabla \cdot \mathbf{B}$ will be zero at any later time so that the $\nabla \cdot \mathbf{B} = 0$ scalar equation is indirectly fulfilled.
- For $\nabla \cdot \mathbf{D}$, the following time evolution equation holds at every space location:

$$(\nabla \cdot \mathbf{D})_t = -\int_0^t (\nabla \cdot \mathbf{J}_s)_{t'}\, dt'. \tag{1}$$

Thus, $\nabla \cdot \mathbf{D}$ may be different from zero at a time t if the integral on the right-hand side of (1) does not vanish. Equation (1) indicates the way in which free charges are introduced by the FDTD algorithm, without explicitly using a charge density function. In the curl equations, in fact, the only allowed physical sources are currents, but not charges.

In order to model an electric dipole of a moment $\mathbf{p} = p_z(t)\hat{\mathbf{e}}_z$ we use one infinitesimal current element (ICE) term $I_s(t)$ [2]. The ICE is associated with a current density $J_s(t)$, located in a E_z grid position indicated by $i_{\rm gap}$, $j_{\rm gap}$, and $k_{\rm gap} + 1/2$. This will also be the position of $\mathbf{p}$. $I_s(t)$ and $p_z(t)$ are related in the following way:

$$p_z(t) = \Delta z \int_0^t I_s(t')\, dt'. \tag{2}$$

For a magnetic dipole of a moment $\mathbf{m} = m_z(t)\hat{\mathbf{e}}_z$, we use four equal ICE terms, forming a loop around the H_z grid point at $i_{\rm loop} + 1/2$, $j_{\rm loop} + 1/2$, and $k_{\rm loop}$ and involving the four nearest $\mathbf{E}$ components, i.e., $E_x(i_{\rm loop} + 1/2, j_{\rm loop}, k_{\rm loop})$, $E_y(i_{\rm loop} + 1, j_{\rm loop} + 1/2, k_{\rm loop})$, $-E_x(i_{\rm loop}+1/2, j_{\rm loop}+1, k_{\rm loop})$, $-E_y(i_{\rm loop}, j_{\rm loop}+1/2, k_{\rm loop})$. $I_s(t)$ and $m_z(t)$ are related as

$$m_z(t) = I_s(t)\Delta x \Delta y. \tag{3}$$

With a $\mathbf{p}$ term, one obtains, for $\nabla \cdot \mathbf{J}_s$, the values $\pm I_s(t)(\Delta x \Delta y \Delta z)^{-1}$ at the grid points above and below the gap, respectively, and zero elsewhere. By setting these values into (1), the following two charges are accumulated, after a time interval T, in the FDTD grid at $(i_{\rm gap}, j_{\rm gap}, k_{\rm gap} + 1)$ and $(i_{\rm gap}, j_{\rm gap}, k_{\rm gap})$, respectively,

$$Q(T) \equiv \Delta x \Delta y \Delta z \nabla \cdot \mathbf{D} = \pm \int_0^T I_s(t)\, dt. \tag{4}$$

If the $I_s(t)$ pulse shape has a nonzero mean value on $[0, T]$, charges in (4) will not disappear at time T. Instead, they actually produce an electric dipole of a moment $Q(T)\Delta z$ with its corresponding static $\mathbf{E}$ field, which is built up after the signal rising front has passed. To prove the FDTD ability in modeling $\mathbf{p}$ or $\mathbf{m}$ static and quasi-static fields, we first apply the so-called triple cosine (TC) [3], a compact nonzero mean value pulse on a time interval $[0, \tau]$. We then introduce the following suitable normalized waveforms:

$$DTC(t) = \tau \frac{d}{dt} TC(t)$$

$$ITC(t) = \frac{1}{\tau} \int_0^\tau TC(t')\, dt'$$

$$IITC(t) = \frac{1}{\tau} \int_0^\tau ITC(t')\, dt'.$$

DTC is a zero mean value compact pulse, ITC is a smoothed step function, and $IITC$ is a ramp function with a smoothed onset (the latter two with a rise time of τ). We use the above waveforms for $I_s(t)$ in (2) and (3) as follows:

- TC to analyze the $\mathbf{p}$-dependent $\mathbf{E}$-field term—the $1/r^3$ electrostatic—by observing E_r and E_θ for $t > \tau$;
- ITC to analyze the $d\mathbf{p}/dt$-dependent $\mathbf{H}$-field term—the $1/r^2$ quasi-static, which is neither radiative, nor electrostatic—by observing H_ϕ for $t > \tau$;

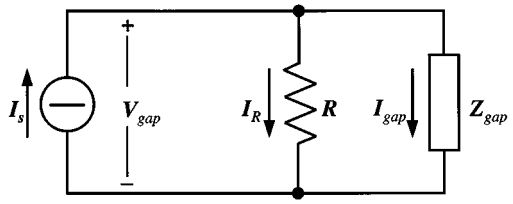

Fig. 1. Circuit model of the source with its internal impedance R.

- ITC to analyze the $\mathbf{m}$-dependent $\mathbf{H}$-field term—the $1/r^3$ magnetostatic such as the one produced by a constant current—by observing H_r and H_θ for $t > \tau$;
- $IITC$ to analyze the $d\mathbf{m}/dt$-dependent $\mathbf{E}$-field term—the $1/r^2$ quasi-static—by observing E_ϕ for $t > \tau$.

Nonradiative $\mathbf{E}$- and $\mathbf{H}$-fields are accurately detectable after $1/r$ radiative contributions have propagated out of the grid. Using a linearly increasing function like $IITC$, the iteration of the FDTD algorithm is stopped before numerical overflow occurs.

III. Avoidance of Static Fields

There are two strategies to prevent static solutions in the FDTD grids. First, the FDTD run can end up with a zero right-hand side in (1), what is ensured by using a zero mean value pulse as introduced in the previous section, or, for example, bipolar pulses proposed in [4]. Second, charges can be dumped using lumped resistors across the grid points where they accumulate [5]. We intend resistor R to be the internal impedance of the source, as in the circuit model of Fig. 1. The lumped resistor is then achieved assuming $\sigma = 1/(\Delta R)$ as conductivity for the $\mathbf{E}$ component corresponding to the ICE (Δ being a cell step size). The source could be the one feeding the gap of a linear antenna, also in the limiting case of a very short dipole of length Δ, i.e., an electric Hertzian dipole (HD) in FDTD. Assuming the potential of the point from which I_s flows out to be positive, the voltage across R is given by

$$V_{\rm gap}(t) = E_{\rm gap}(t)\Delta \tag{5}$$

where we define $E_{\rm gap}$ as the reversed $\mathbf{E}$ component corresponding to the ICE. By Fig. 1, the corresponding gap current is then

$$I_{\rm gap} = I_s - I_R = I_s - \sigma E_{\rm gap}\Delta^2. \tag{6}$$

The use of (6) is direct and avoids $\mathbf{H}$ line integration around the gap, a technique which is usually adopted in the FDTD method to obtain currents. We emphasize that counterclockwise (with respect to the positive reference orientation of the ICE) line integration does not give $I_{\rm gap}$ directly, but rather a total current $I_{\rm tot}$ including a displacement contribution

$$I_{\rm tot} = I_{\rm gap} + I_{\rm disp} = I_{\rm gap} - \varepsilon_r \varepsilon_o \frac{dE_{\rm gap}}{dt} \Delta^2. \tag{7}$$

To avoid problems of the kind reported in [6], the $I_{\rm disp}$ term should be subtracted from the "measured" current $I_{\rm tot}$.

IV. Results

Dipoles were implemented in a $80 \times 160 \times 160$ cubical grid and located along the z-axis on a symmetry plane perpendicular to the x-axis. The cell size Δ was 2.5 mm and the time step was $\Delta t = \Delta/(2c) \cong 4.166$ ps. Absorbing boundary conditions (ABCs) were second-order Higdon [7]. The pulse duration τ was $(1.8\ \text{GHz})^{-1} \cong 0.555$ ps. Waves took 1.15 ns, or approximately 2τ, to reach the farthest boundary points and, consequently, an overall simulation time $T = 4\tau$ was used. Fig. 2

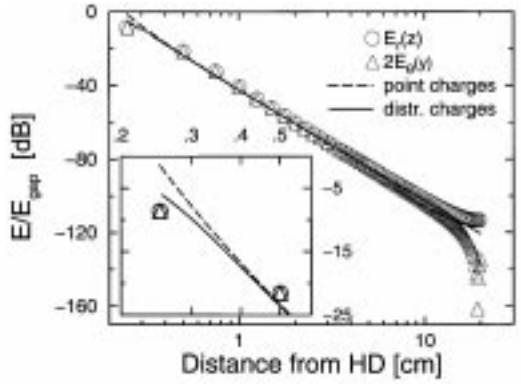

Fig. 2. FDTD results (open symbols) versus analytic solutions (solid and dashed lines) for $\mathbf{p}$. The slope is -60 dB/decade, i.e., a $1/r^3$ law for E_θ and E_r. The subplot is an enlarged view of the region within two cell step sizes from the source.

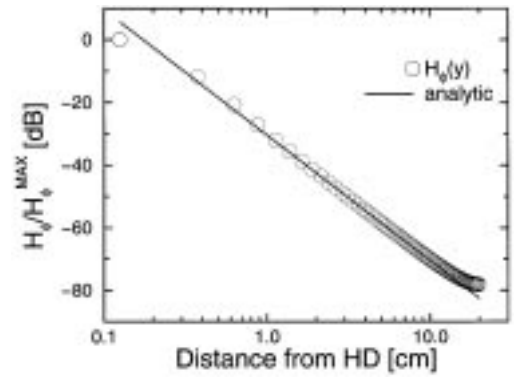

Fig. 3. FDTD results (open symbols) versus analytic solution (solid line) for $d\mathbf{p}/dt$. The slope is -40 dB/decade, i.e., a $1/r^2$ law for H_ϕ.

shows residual values of the $1/r^3$ static $\mathbf{E}$-field for $\mathbf{p}$ (relevant field components are indicated as spherical coordinate components). The accumulated charge evaluated from (4) amounted to 174.6111 pC. The dashed line represents the field of two point charges of such a value, while the solid line refers to uniform distributions in a volume Δ^3. Similar to [2], FDTD results deviate from the analytic ones within five cells off the dipole and fit neither the point, nor the distributed charge field values. This is due to the coarse spatial sampling of the grid close to $\mathbf{p}$.

Fig. 2 also shows the ABC's inability to deal with static fields: starting from $\sim$10 cm to the boundary, fields deviate from expected values in different ways. Although this is not evident on a logarithmic scale, E_θ tends to linearly decrease, even changing sign at the boundary, E_r tends to become a constant. In fact, when in the second-order ABC's equation, the temporal derivative vanishes and only a linear or constant spatial dependence is allowed.

Deviations from analytic solutions are five orders of magnitude lower than the field between the dipole charges, e.g., $E_{\rm gap}$ taken as a reference. This value can be deduced *a priori* by applying grid symmetry considerations and the Gauss theorem in a discrete form on the faces of a cubic cell of edge Δ centered around a charge

$$Q = 3\varepsilon_o E_{\rm gap}\Delta^2. \tag{8}$$

Fig. 3 shows the $1/r^2\mathbf{H}$ normalized field with the simulation arranged to emphasize the $d\mathbf{p}/dt$ term of the electric dipole. Figs. 4 and 5 show the $\mathbf{m}$ and $d\mathbf{m}/dt$ normalized contributions of the magnetic dipole, respectively. Previous remarks on the fields' dependence still hold in these cases. Tables I and II prove charge and energy conservation to be satisfied by the algorithm. The energy (although in a

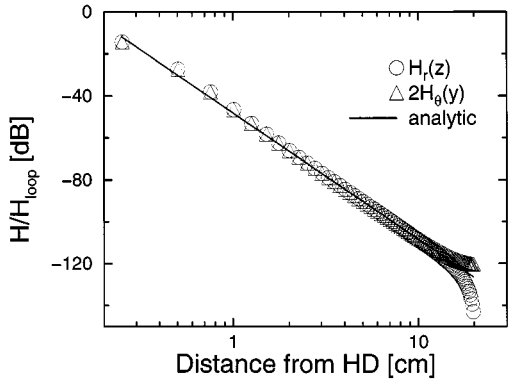

Fig. 4. FDTD results (open symbols) versus analytic solutions (solid line) for $\mathbf{m}$. The slope is -60 dB/decade, i.e., a $1/r^3$ for H_θ and H_r.

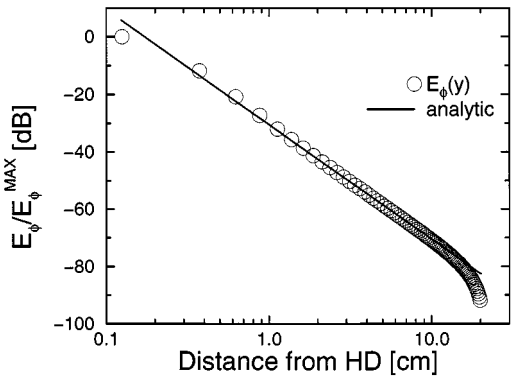

Fig. 5. FDTD results (open symbols) versus analytic solution (solid line) for $d\mathbf{m}/dt$. The slope is -40 dB/decade, i.e., a $1/r^2$ law for E_ϕ.

TABLE I
ELECTRIC CHARGE CONSERVATION FOR $\mathbf{p}$ (STATIC CASE)

Method of calculation	Calculated charge
$\int_0^T TC(t)\,dt$	173.6111 pC
$Q = 3\varepsilon_o E_{gap}\Delta^2$	173.6111 pC

TABLE II
ENERGY CONSERVATION FOR $\mathbf{p}$ (STATIC CASE)

Method of calculation	Calculated energy
$\frac{1}{2}\varepsilon_o \iiint_V E^2(T)\,dV$	226.9407 nJ
$\int_0^T \iint_S \mathbf{E}(t)\times\mathbf{H}(t)\cdot d\mathbf{S}\,dt$	0.0181 nJ
$\int_0^T V_{gap}(t) I_{gap}(t)\,dt$	226.9605 nJ

closed structure) and charge conservation properties can also be shown to hold by an algebraic proof [8]. Table I compares electric charge as calculated, in two independent ways, from (4) and (8). Table II compares contributions of space stored energy, energy radiated trough the grid boundaries, and energy injected directly by the source. The latter must equal the sum of the first two. $V_{\rm gap}(t)$, evaluated from (5), is the electromotive force (EMF) along the ICE ($I_s = I_{\rm gap}$ and DTC is

TABLE III
ENERGY CONSERVATION FOR $\mathbf{m}$ (STATIC CASE)

Method of calculation	Calculated energy
$\frac{1}{2}\mu_o \iiint_V H^2(T)\,dV$	102.2655 pJ
$\int_0^T \iint_S \mathbf{E}(t)\times\mathbf{H}(t)\cdot d\mathbf{S}\,dt$	0.0041 pJ
$\int_0^T V_{loop}(t) I_s(t)\,dt$	102.2695 pJ

TABLE IV
POWER BALANCE FOR $\mathbf{p}$ AT 1.8 GHz. $I_{\rm gap} = 1$ A

Method of calculation	Calculated power
$\frac{1}{12\pi}\sqrt{\frac{\mu_o}{\varepsilon_o}}\left(\frac{\omega\Delta}{c}\right)^2 \lvert I_{gap}(\omega)\rvert^2$	88.88 mW[(a)]
$\frac{1}{12}\mathrm{Re}\iint \mathbf{E}_\omega\times\mathbf{H}^*_\omega\cdot d\mathbf{S}$	88.97 mW[(b)] 88.83 mW[(c)]
$\frac{1}{2}\mathrm{Re}\left[V_{gap}(\omega) I^*_{gap}(\omega)\right]$	88.94 mW[(b)] 88.02 mW[(c)]

(a) analytic result. *(b)* resistor. *(c)* zero mean value pulse.

used instead of a lumped resistor). Table III shows the same balance for $\mathbf{m}$. Here, $V_{\rm loop}(t)$, calculated using E_ϕ, is the EMF along the current loop. Finally, Table IV shows, for $\mathbf{p}$, a balance in the frequency domain (1.8 GHz) between the source power and corresponding flux leaving the grid boundaries. To avoid static fields, both methods described above are used. Calculated data are compared to the analytic value of the power delivered by an ICE of the same length (first row). The observed deviation is within 0.15%; a figure that would not be reached without using methods to prevent static fields. If these fields are not removed in accordance with the techniques suggested here, special post-processing of data [9], [10] is needed. Otherwise, an instability is produced by Fourier transforming, even when time-domain fields' values converge satisfactorily.

V. CONCLUSIONS

Apart from high-frequency applications, the FDTD method is also capable of solving static problems. The nonrecognition of this ability has led some investigators to consider such solutions, which may cause serious problems in the frequency domain, as numerical artifacts. In this paper, besides proposing techniques to eliminate them, we have presented the possibility of using the FDTD method in static and quasi-static calculations (electric and magnetic dipoles). However, it has not yet been determined if the FDTD method can efficiently compete with consolidated scalar techniques because it typically still involves an excessive number of time steps needed to attain acceptable solutions.

REFERENCES

[1] K. S. Yee, "Numerical solution of initial boundary value problems involving Maxwell's equations in isotropic media," *IEEE Trans. Antennas Propagat.*, vol. AP-17, pp. 585–589, 1966.

[2] D. N. Buechler, D. H. Roper, C. H. Durney, and D. A. Christensen, "Modeling sources in the FDTD formulation and their use in quantifying source and boundary condition errors," *IEEE Trans. Microwave Theory Tech.*, vol. 43, pp. 810–814, Apr. 1995.

[3] T. G. Moore, J. G. Blaschack, A. Taflove, and G. A. Kriegsmann, "Theory and application of radiation boundary operators," *IEEE Trans. Antennas Propagat.*, vol. 36, pp. 1797–1812, Dec. 1988.

[4] C. M. Furse, D. H. Roper, D. N. Buechler, D. A. Christensen, and C. H. Durney, "The problem and treatment of DC offsets in FDTD simulations," *IEEE Trans. Antennas Propagat.*, vol. 48, pp. 1198–1201, Aug. 2000.

[5] A. Reineix and B. Jecko, "Analysis of microstrip patch antennas using finite difference time domain method," *IEEE Trans. Antennas Propagat.*, vol. 37, pp. 1361–1369, Nov. 1989.

[6] K. A. Chamberlain, J. D. Morrow, and R. J. Luebbers, "Frequency-domain and finite-difference, time-domain solutions to a nonlinearally-terminated dipole: Theory and validation," *IEEE Trans. Electromagn. Compat.*, vol. 34, pp. 416–422, Nov. 1992.

[7] R. L. Higdon, "Absorbing boundary conditions for difference approximations to the multidimensional wave equation," *Math. Comput.*, vol. 47, no. 176, pp. 437–459, Oct. 1986.

[8] P. Thoma and T. Weiland, "Numerical stability of finite difference time domain methods," *IEEE Trans. Magn.*, vol. 34, pp. 2740–2743, Sept. 1998.

[9] C. M. Furse, S. P. Matur, and O. P. Gandhi, "Improvements to the finite-difference time-domain method for calculating the radar cross section of a perfectly conducting target," *IEEE Trans. Microwave Theory Tech.*, vol. 38, pp. 919–927, July 1990.

[10] U. Kangro and R. Nicolaides, "Spurious fields in time-domain computations of scattering problems," *IEEE Trans. Antennas Propagat.*, vol. 45, pp. 228–234, Feb. 1997.

An Improved Algorithm of Constructing Potentials From Cauchy Data and Its Application in Synthesis of Nonuniform Transmission Lines

Gaobiao Xiao and Ken'ichiro Yashiro

***Abstract*—It is required to construct a potential function from Cauchy data in the synthesis of arbitrarily terminated nonuniform transmission lines. An improved algorithm for this problem is discussed in this paper. With the proposed algorithm, not only is computation time reduced, but the possible divergence of the potential function that sometimes occur when adopting the successive approximation method is also avoided. It has been applied successfully to designs of nonuniform transmission-line filters or tapers through solving inverse problems.**

***Index Terms*—Filter, inverse problem, nonuniform transmission lines.**

I. INTRODUCTION

The synthesis of nonuniform transmission lines (NTLs) has been investigated by many authors [1]–[4] and, among them, the methods based on solving inverse scattering problems are probably most promising. We have proposed a numerical method to synthesize arbitrarily terminated NTLs by solving a related inverse classic

Manuscript received May 14, 2001.

G. Xiao is with the Graduate School of Science and Technology, Chiba University, Chiba City 263-8522, Japan and also with the Faculty of Electronics and Information, Hunan University, Hunan 410082, China.

K. Yashiro is with the Faculty of Engineering, Chiba University, Chiba City 263-8522, Japan.

Publisher Item Identifier 10.1109/TMTT.2002.801382.